Intraligand Charge Transfer in $Pt(qol)_2$. Characterization of Electronic States by High-Resolution Shpol'skii Spectroscopy

Dirk Donges,[†] Jeffrey K. Nagle,[‡] and Hartmut Yersin*[,†]

Institut für Physikalische und Theoretische Chemie, Universität Regensburg, D-93040 Regensburg, Germany, and Department of Chemistry, Bowdoin College, Brunswick, Maine 04011

Received August 5, 1996[⊗]

$Pt(qol)_2$ ($qol^- =$ 8-quinolinolato-*O,N*) is investigated in the Shpol'skii matrices *n*-heptane, *n*-octane-h_{18}, *n*-octane-d_{18}, *n*-nonane, and *n*-decane, respectively. For the first time, highly resolved triplet phosphorescence as well as triplet and singlet excitation spectra are obtained at $T = 1.2$ K by site-selective spectroscopy. This permits the detailed characterization of the low-lying singlet and triplet states which are assigned to result mainly from intraligand charge transfer (ILCT) transitions. The electronic origin corresponding to the ^{3}ILCT lies at 15 426 cm^{-1} (FWHM ≈ 3 cm^{-1}) exhibiting a zero-field splitting smaller than 1 cm^{-1}, which shows that the metal d-orbital contribution to the ^{3}ILCT is small. At $T = 1.2$ K, the three triplet sublevels emit independently due to slow spin−lattice relaxation (slr) processes. Therefore, the phosphorescence decays triexponentially with components of 4.5, 13, and 60 μs. Interestingly, two of the sublevels can be excited selectively, which leads to a distinct spin polarization manifested by a biexponential decay. At $T = 20$ K, the decay becomes monoexponential with $\tau = 10$ μs due to a fast slr between the triplet sublevels. From the Zeeman splitting of the ^{3}ILCT the *g*-factor is determined to be 2.0 as expected for a relatively pure spin triplet. The ^{1}ILCT has its electronic origin at 18 767 cm^{-1} and exhibits a homogeneous line width of about 12 cm^{-1}. This feature allows us to estimate a singlet−triplet intersystem crossing rate of about 2×10^{12} s^{-1}. This relatively large rate compared to values found for closed shell metal $M(qol)_n$ compounds displays the importance of spin−orbit coupling induced by the heavy metal ion. Moreover, this small admixture leads to the relatively short emission decay times. All spectra show highly resolved vibrational satellite structures. These patterns provide information about vibrational energies (which are in good accordance with Raman data) and shifts of equilibrium positions between ground and excited states. These shifts are different in the ^{1}ILCT and ^{3}ILCT states. The vibrational satellite structures support the assignment of ILCT character to the lowest excited states.

1. Introduction

Coordination compounds of the ubiquitous ligand 8-quinolinolato-*O,N* (qol^-) have long found use in spectrophotometric analyses of metal ions.[1,2] In addition, photoluminescence[3−6] and electroluminescence[7,8] have been observed in several diamagnetic compounds of qol^-. Recently, electroluminescence from $Al(qol)_3$ has been shown to play a crucial role in the development of white-light-emitting "organic electroluminescent devices" (OLEDs). Such devices may represent building blocks for next-generation flat panel display systems.[8] While many compounds of main group metals with qol^- ligands, including $Al(qol)_3$, exhibit an intense and short-lived green fluorescence, other complexes, like $Pt(qol)_2$, show very intense red phosphorescence, even in solution at room temperature.[3] In particular, the latter compound has been used as a redox photosensitizer for electron transfer reactions in solar energy conversion processes and for other photocatalytic applications involving its low-lying excited electronic states.[9,10] Moreover, $Pt(qol)_2$ exhibits a strong absorption band which lies unusually low relative to other 8-quinolinol compounds. These features make $Pt(qol)_2$ an outstanding candidate for further investigations.

Surprisingly little is known about the details of the electronic structure of the aforementioned metal compounds of qol^- and the nature of the electronic states involved in the low energy absorption and emission bands. One reason for this lack of information is that the optical absorption and emission spectra available are very broad (half-widths of $\approx$2000 cm^{-1}), thus slurring all details. However, if one obtains highly resolved spectra, a much deeper understanding of the electronic characteristics of the compound is possible. This has been demonstrated recently for other transition metal complexes if doped into suitable crystalline matrices.[11−16] In the present investigation, it is intended to apply such methods also to

[†] Universität Regensburg.
[‡] Bowdoin College.
[⊗] Abstract published in *Advance ACS Abstracts,* June 1, 1997.

(1) Hollingshead, R. G. W. *Oxine and its Derivatives*; Butterworths: London, 1954−1956; Vols. I−IV.
(2) Sandell, E. B.; Onishi, H. *Photometric Determination of Traces of Metals*, General Aspects; Fourth Edition of Part I of *Colorimetric Determination of Traces of Metals*; Wiley: New York, 1978; pp 415−448.
(3) Ballardini, R.; Varani, G.; Indelli, M. T.; Scandola, F. *Inorg. Chem.* **1986**, *25*, 3858.
(4) Bartocci, C.; Sostero, S.; Traverso, O.; Cox, A.; Kemp, T. J.; Reed, W. J. *J. Chem. Soc., Faraday Trans.* **1980**, *76*, 797.
(5) Ballardini, R.; Indelli, M. T.; Varani, G.; Bignozzi, C. A.; Scandola, F. *Inorg. Chim. Acta* **1978**, *31*, L423.
(6) Becker, R. S. *Theory and Interpretation of Fluorescence and Phosphorescence*; Wiley: New York, 1969; pp 199−201.
(7) Vogler, A.; Kunkely, H. In *High-Energy Processes in Organometallic Chemistry*; Suslick, K., Ed.; ACS Symposium Series 333; American Chemical Society: Washington, DC, 1987; pp 155−168.
(8) Kido, J.; Kimura, M.; Nagai, K. *Science* **1995**, *267*, 1332.
(9) Scandola, F.; Ballardini, R.; Indelli, M. T. In *Photochemical and Photoelectrochemical and Photobiological Processes, Solar Energy R & D Eur. Comm. Ser. D*; Hall, D. O., Ed.; Kluwer: Dordrecht, The Netherlands, 1982; p 66.
(10) Borgarello, E.; Pelizzetti, E.; Ballardini, R.; Scandola, F. *Nouv. J. Chim.* **1984**, *8*, 567.
(11) Humbs, W.; Yersin, H. *Inorg. Chem.* **1996**, *35*, 2220.
(12) Yersin, H.; Humbs, W.; Strasser, J. In *Electronic and Vibronic Spectra of Transition Metal Complexes, Vol. II*; Yersin, Ed.; Topics in Current Chemistry 191; Springer Verlag: Berlin, 1997; p 153.

S0020-1669(96)00946-9 CCC: $14.00

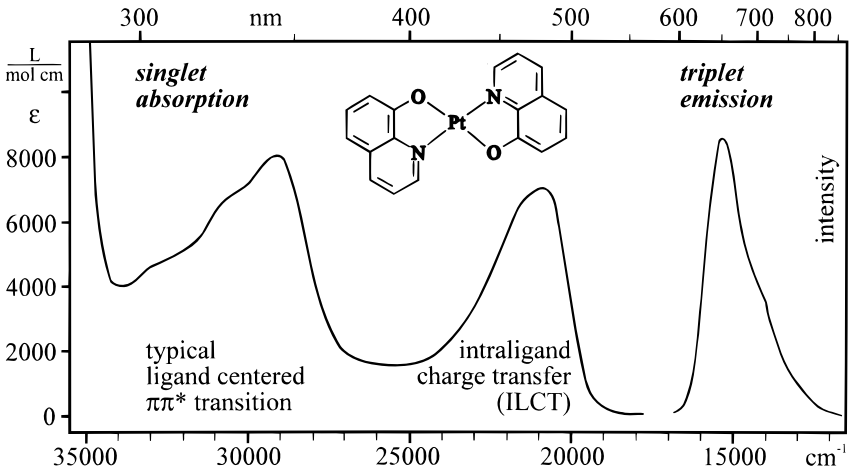

Figure 1. Room temperature absorption and emission spectra of $Pt(qol)_2$ in DMF. (Compare also to ref 1.)

$Pt(qol)_2$. Since this compound is planar and uncharged and does not possess a permanent dipole moment (*trans* configuration, see inset of Figure 1), $Pt(qol)_2$ appears to be a good candidate for applying the Shpol'skii matrix isolation technique. This method is well established for organic molecules[17,18] and recently also for an interesting class of planar cyclometalated compounds.[13,14,19,20] In this technique, a chromophore is dissolved in an *n*-alkane solvent which at low temperature forms a polycrystalline matrix. The chromophores substitute for host molecules and occupy well-defined guest sites. If guest and host possess at least *similar* geometries, often only small distortions of the guest are induced.

Indeed, $Pt(qol)_2$ fulfills these conditions.[21] Therefore, highly resolved spectra of this compound are obtained for the first time. This information is used for a detailed characterization of the lowest excited singlet and triplet states. In particular, it is intended to assign the orbital character of these states, to obtain information about changes of force constants and equilibrium positions of the potential hypersurfaces upon excitation, and to focus on interesting decay properties connected to the sublevels of the lowest triplet state.

2. Experimental Section

Samples of $Pt(qol)_2$ were prepared according to the two different procedures described in refs 3 and 5, respectively. 8-Quinolinol was reagent grade (Merck), and $K_2[PtCl_4]$ (Aesar) was of 99.9% purity. No differences in spectroscopic properties were observed between samples prepared according to the two procedures. The product samples were washed with dilute acetic acid, ethanol, and dichloromethane followed by recrystallization from either *N*,*N*-dimethylformamide (DMF) or 1,4-dioxane and washed again with *n*-octane. Since $Pt(qol)_2$ is photochemically labile in the presence of dissolved oxygen,[3,4] solutions were prepared in the dark as much as possible.

Since $Pt(qol)_2$ is not soluble in *n*-alkanes, it was first dissolved in a solvent of intermediate polarity (1,4-dioxane) and subsequently diluted with the respective *n*-alkane. All solvents were of the highest available commercial grade. The volume ratio of 1,4-dioxane to *n*-alkane was 1:50, yielding a $Pt(qol)_2$ concentration of 10^{-5} mol/L. After filling quartz cells of 2 mm diameter, the solutions were frozen at a cooling rate of about 100 K/min.

Details of the experimental equipment[11,14] and the optical setup[24] are described elsewhere.

3. Results and Discussion

3.1. Room Temperature Spectra and Types of Transitions. Figure 1 gives a survey of the room temperature absorption and emission spectra of $Pt(qol)_2$ dissolved in DMF. These spectra largely correspond to those previously published.[2,3]

The high-energy absorption near 29 000 cm^{-1} (345 nm, $\epsilon \approx$ 8000 L mol^{-1} cm^{-1}) is typical also for many other metal chelates with 8-quinolinolato ligands, like $Al(qol)_3$ and $Rh(qol)_3$. Mainly from this feature and the small solvatochromism observed for these complexes it was concluded in ref 3 that this absorption can be assigned to typical ligand-centered transitions of $\pi\pi^*$ character.

The low-energy absorption of $Pt(qol)_2$ near 21 000 cm^{-1} (478 nm, $\epsilon \approx$ 6900 L mol^{-1} cm^{-1}) was also assigned to a ligand-centered transition, since a corresponding transition appears for the uncoordinated ligand as well as for $Al(qol)_3$ and $Rh(qol)_3$, for example. The unsubstituted heterocycle quinoline does not exhibit an equivalent absorption.[3] From investigations with uncoordinated quinolinol (pH dependence of the absorption energy, solvatochromism) it was concluded that the corresponding absorption band results from a transfer of electron charge density from the oxygen to the nitrogen, or from the phenolic side to the pyridyl part of the quinolinol ring system.[25−28] The near correspondence of the absorption band of the uncoordinated ligand with those of the complexes leads to the suggestion that the same type of transition occurs also in the metal compounds.[3] Therefore, this strong low-energy absorption is assigned to a singlet intraligand charge transfer (^{1}ILCT) transition. (This notation, first introduced by Vogler et al.[29] for a different compound, seems to characterize the situation well. It corre-

(13) Yersin, H.; Schützenmeier, S.; Wiedenhofer, H.; von Zelewsky, A. *J. Phys. Chem.* **1993**, *97*, 13496.
(14) Wiedenhofer, H.; Schützenmeier, S.; von Zelewsky, A.; Yersin, H. *J. Phys. Chem.* **1995**, *99*, 13385.
(15) Colombo, M. G.; Hauser, A.; Güdel, H. U. In *Electronic and Vibronic Spectra of Transition Metal Complexes, Vol. 1, Top. Curr Chem. 171*; Yersin, H., Ed.; Springer: Berlin, Germany, 1994; p 143.
(16) Zilian, A.; Güdel, H. U. *Inorg. Chem.* **1992**, *31*, 830.
(17) Shpol'skii, E. V. *Sov. Phys. Usp. (Engl. Transl.)* **1960**, *3*, 372.
(18) Palewska, K.; Lipinski, J.; Sworakowski, J.; Sepiol, J.; Gygax, H.; Meister, E. C.; Wild, U. P. *J. Phys. Chem.* **1995**, *99*, 16835.
(19) Becker-Donges, D.; Yersin, H.; von Zelewsky, A. *Chem. Phys. Lett.* **1995**, *235*, 490.
(20) Schmidt, J.; Wiedenhofer, H.; von Zelewsky, A.; Yersin, H. *J. Phys. Chem.* **1995**, *99*, 226.
(21) $Pt(qol)_2$ has a length of about 1.25 nm along its long axis (ref 22) and thus fits well to *n*-octane (with a length of 1.26 nm, ref 23).
(22) Bergamini, P; Bertolasi, V.; Ferretti, V.; Sostero, S. *Inorg. Chim. Acta* **1987**, *126*, 151.
(23) Nakhimovsky, L. A.; Lamotte, M.; Joussot-Dubien, J. *Handbook of Low Temperature Electronic Spectra of Polycyclic Aromatic Hydrocarbons*; Elsevier Science Publishers: Amsterdam, 1989.
(24) Stock, M.; Yersin, H. *Chem. Phys. Lett.* **1976**, *40*, 423.
(25) Bailey, A. S.; Williams, R. J. P.; Wright, J. D. *J. Chem. Soc.* **1965**, 2579.
(26) Goldman, M.; Wehry, E. L. *Anal. Chem.* **1970**, *42*, 1178.
(27) Burton, R. E.; Davis, W. J. *J. Chem. Soc.* **1964**, 1766.
(28) Bardez, E.; Chatelain, A.; Larrey, B.; Valeur, B. *J. Phys. Chem.* **1994**, *98*, 2357.
(29) Vogler, A.; Kunkely, H. *Inorg. Chim. Acta* **1981**, *54*, L 273.

sponds to the notation of lone-pair-π^* ($l\pi^*$)[30] applied by Scandola and co-workers.[3]) Independently, an analogous assignment was proposed for the similar $Pt(qtl)_2$ ($qtl^- = 8$-quinolinethiolato-*N*,*S*).[31]

An alternative assignment of the low-energy absorption band of $Pt(qol)_2$ is not very likely, since (i) LMCT transitions should lie at much higher energies, especially for Pt(II) compounds;[3,32] (ii) dd*-MC transitions would be much weaker, and the corresponding energies are expected to lie above $\approx$26 000 cm^{-1} (compare refs 33 and 34); and (iii) MLCT transitions, which might occur in that energy range in $Pt(qol)_2$, can be ruled out due to the occurrence of the equivalent absorption bands also in closed shell metal compounds like $Al(qol)_3$. These compounds are unlikely to exhibit such a low-energy MLCT transition (for example, see ref 3). The detailed discussion in the following sections will also show that an assignment as an MLCT transition can be excluded.

The emission shown in Figure 1 (15 400 cm^{-1}, 650 nm) has a relatively long lifetime even at $T = 298$ K ($\tau \approx 3$ μs). Therefore, this luminescence can be classified as phosphorescence from the lowest excited triplet to the singlet ground state. Since no singlet fluorescence (from the ^{1}ILCT) could be observed, in contrast to $Al(qol)_3$, it was concluded that $Pt(qol)_2$ exhibits an efficient intersystem crossing.[3] Various assignments of the MO parentage of the triplet state have been proposed, but the issue remains unresolved. While a dd* transition was initially suggested,[4] subsequent workers[3] considered two interpretations of ligand-centered transitions ($^3\pi\pi^*$ or ^{3}ILCT). The amount of metal perturbation could not be specified.

More information about the nature of the lowest excited states and the extent of metal involvement in these electronic transitions is required. Unfortunately, the large half-widths of the bands observed precludes their use in a more detailed characterization. However, the required information may be obtained from highly resolved spectra as shown below.

3.2. Different Shpol'skii Matrices. $Pt(qol)_2$ is investigated in the Shpol'skii matrices *n*-heptane, *n*-octane-h_{18}, *n*-octane-d_{18}, *n*-nonane, and *n*-decane, respectively. It exhibits an intense red luminescence at low temperatures. The chromophores occupy different guest sites in each matrix, which leads to superimposed quasi-line spectra. However, by site-selective spectroscopic methods these spectra may be separated from each other (see below). In all matrices, three or four intensely emitting sites with line half-widths (FWHM) between 2.5 and 3.5 cm^{-1} were found. Thus, the spectral resolution is about 400 times better than so far published. The energy positions of the electronic origins assigned to the lowest triplet (see also section 3.4) are listed in Table 1. The origins of the different sites are observed in a range of about 150 cm^{-1} for one specific matrix and cover about 230 cm^{-1} when the different *n*-alkanes investigated are compared.

Besides the well-resolved electronic origins, the Shpol'skii spectra exhibit highly resolved vibrational satellite structures (section 3.4). As examples, Table 1 shows the energies of the dominant vibrational modes for each site. A weak dependence of the energy on the site is observed.

For further investigations, the site with lowest energy in *n*-octane was selected. For this site, the electronic origin of the phosphorescence is located at 15 426 cm^{-1}. In particular, this site will be separated by selectively detected excitation or selectively excited emission spectra.

Table 1. Emission Data of $Pt(qol)_2$ in Different Shpol'skii Matrices

matrix[a]	triplet origin of dominant sites[b] (cm^{-1})	rel intensity[c] (%)	Pt−N vibration[d] (cm^{-1})	Pt−O vibration[d] (cm^{-1})
n-heptane	15 473	100	245	413
	15 487	100	245	413
	15 630	75	251	414
***n*-octane-h_{18}[e]**	**15 426**	**88**	**253**	**413**
	15 507	100	248	412
	15 517	35	249	413
	15 568	65	250	413
n-octane-d_{18}[f]	15 437	25	254	412
	15 518	100	251	414
	15 571	49	254	415
	15 616	5	252	414
n-nonane	15 420	100	248	413
	15 448	47	249	413
	15 572	24	249	414
n-decane	15 403	100	246	412
	15 426	100	246	412
	15 534	15	251	412

[a] 1,4-Dioxane was used as intermediate solvent. Nominal concentration of the complex 10^{-5} M. [b] $T = 5.0$ K. Excitation at 488.0 nm ($\approx$20 490 cm^{-1}). Only sites that contribute more than 5% to the total emission intensity are considered (accuracy ± 1 cm^{-1}). The line half-widths (fwhm) lie between 2.5 and 3.5 cm^{-1} for all sites. [c] Accuracy $\pm$5%. [d] Largest atomic displacements of the respective atoms in the corresponding normal mode (see section 3.3). The energy is measured relative to the respective electronic origin (see also Table 3; accuracy ± 1 cm^{-1}). [e] This site will mainly be investigated in this contribution. [f] Perdeuterated *n*-octane.

3.3. Site-Selective Excitation Spectra of the Lowest Excited Singlet State. Figure 2a shows the singlet excitation spectrum of $Pt(qol)_2$ measured at $T = 1.2$ K. The emission was detected at the 15 426 cm^{-1} triplet origin (see Table 1). Thus, the singlet corresponding to that site is selectively registered. In the energy range from 16 300 cm^{-1} to 18 700 cm^{-1}, no further excitation peak could be detected. Moreover, in the range from $\approx$21 500 cm^{-1} to $\approx$24 000 cm^{-1}, no sharp lines were found (spectrum not reproduced). Therefore, the singlet excitation is very likely correlated with the broad ^{1}ILCT absorption in DMF having its maximum near 21 000 cm^{-1} (Figure 1). The fact that the excitation spectrum lies at somewhat lower energy is mainly due to the much less polar character of *n*-octane than that of DMF. The change of the envelope from the broad spectrum to the site-selectively excited one is attributed to the enormously reduced spread of inhomogeneously distributed chromophores in the Shpol'skii matrix.

Electronic Origin. The peak of lowest energy located at (18 767 $\pm$ 1) cm^{-1} (532.85 nm) is assigned as electronic origin (Figure 2a). It is connected with a large number of vibrational satellites (progressions and combinations, see below). This assignment as origin is supported not only by the fact that it is the peak of lowest energy in that energy range but also by the fact that the whole vibrational satellite structure can only be fitted to this peak. For example, the progressions of the 253 cm^{-1} and the 413 cm^{-1} modes (see also below) have just this peak as a common origin.

For completeness, one should exclude the possibility that the excitation spectrum is due to a triplet excitation. In this case, the application of a high magnetic field would result in a distinct change of the spectrum. Figure 2b shows the origin range of the excitation spectrum for $B = 0$, 6, and 12 T ($T = 1.5$ K). There is no perceptible variation in the spectrum, neither a Zeeman splitting, a spectral shift, a change of line width, a change in intensity, nor a growing in of additional peaks. This

(30) Kasha, M.; Rawls, H. R. *Photochem. Photobiol.* **1968**, *7*, 561.
(31) Zuika, I. V.; Bruveris, Z. P. *Koord. Khim.* **1979**, *5*, 1390; *Sov. Coord. Chem.* **1979**, *5*, 1083.
(32) Maestri, M.; Sandrini, D.; Balzani, V.; von Zelewsky, A.; Deuschel-Cornioley, C.; Jolliet, P. *Helv. Chim. Acta* **1988**, *71*, 1053.
(33) Lever, A. B. P. *Inorganic Electronic Spectroscopy*, 2nd ed.; Elsevier Publishers: Amsterdam, The Netherlands, 1984; p 550.
(34) Fenske, R. F.; Martin, D. S., Jr.; Ruedenberg, K. *Inorg. Chem.* **1962**, *1*, 441.

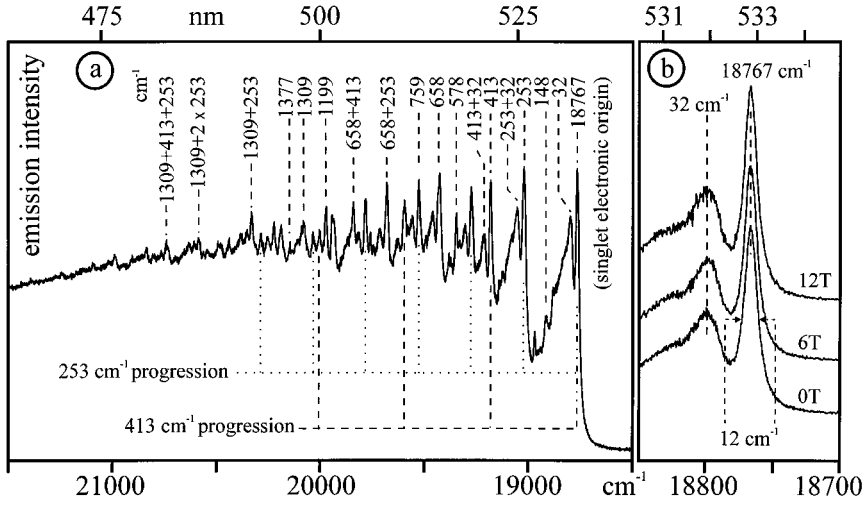

Figure 2. (a) Singlet (^{1}ILCT) excitation spectrum of $Pt(qol)_2$ in an *n*-octane Shpol'skii matrix at $T = 1.2$ K. Due to the selective detection at 15 426 cm^{-1} (electronic origin of the ^{3}ILCT state) a specific site is investigated. Spectral resolution: 0.9 cm^{-1}. The vibrational satellites are specified relative to the electronic origin at 18 767 cm^{-1} (see Table 2). Progressions of the 253 and 413 cm^{-1} modes are connected by dotted and broken lines, respectively. The spectrum is not corrected with respect to the characteristics of the laser dyes (coumarin 102 and 307). (b) Excitation spectra in the range of the singlet origin (expanded) for different magnetic fields ($T = 1.5$ K).

fact is proof of the singlet character of the involved state (^{1}ILCT).

The spectral shape of the singlet origin at 18 767 cm^{-1} can be well fitted by a Lorentzian line shape, while a Gaussian fit may be excluded.[35] This is a very interesting result, since it allows one to conclude that the spectral line width of the electronic origin is *homogeneously* determined (for example, see ref 36) but *not* given by an inhomogeneous broadening which results from slightly different environments of the chromophores. Thus, applying the Heisenberg uncertainty principle $\Delta E\,\tau \approx h/2\pi$ (with $\Delta E = hc\Delta\nu$, $\Delta\nu$ = experimentally determined FWHM, h = Planck's constant), one can estimate the lifetime τ of that ^{1}ILCT state. With $\Delta\nu = 12$ cm^{-1} (Figure 2b) one obtains a lifetime of $\tau \approx 5 \times 10^{-13}$ s (corresponding to a rate of $k \approx 2 \times 10^{12}$ s^{-1}). With respect to the large efficiency of intersystem crossing (isc) from the ^{1}ILCT to the emitting triplet ($\eta_{isc} \approx 0.9$ at room temperature[3]), it can be concluded that the lifetime is mainly determined by this isc process. A similar value ($k_{isc} \approx 3 \times 10^{12}$ s^{-1}) was deduced for the lowest excited singlet of Pt(II) porphine.[37] For comparison, the radiative fluorescence rate (^{1}ILCT → ground state) can be estimated from the allowedness of the corresponding ^{1}ILCT absorption band (Figure 1) to be $k_{rad} \approx 2 \times 10^7$ s. Thus, for $Pt(qol)_2$ the rate of isc is about 5 orders of magnitude larger than the radiative decay rate. On the other hand, compounds like $Al(qol)_3$ fluoresce but do not show any phosphorescence.[3] In this case, the rate of isc from ^{1}ILCT to the lower lying triplet can be neglected because it is significantly smaller than the radiative decay rate of the ^{1}ILCT. Obviously, the relatively high isc rate for $Pt(qol)_2$ can be ascribed to the importance of the higher spin−orbit coupling constant of the transition metal compared to closed shell metal ions and a distinct Pt 5d-orbital admixture.

The singlet excitation of $Pt(qol)_2$ measured in the perdeuterated *n*-octane-d_{18} matrix yielded a spectrum very similar to the one measured in protonated *n*-octane-h_{18}. The singlet origin occurs at 18 780 cm^{-1} for the site having its triplet origin at 15 437 cm^{-1} (detection line, see Table 1).[38] The fact that the energy difference between singlet and triplet, which is essentially determined by the exchange interaction, remains almost the same for the different matrices confirms the relatively weak influence of the matrix on the chromophore. The values of the singlet−triplet energy differences are (3341 ± 2) cm^{-1} in *n*-octane-h_{18} and (3344 ± 2) cm^{-1} in *n*-octane-d_{18}.

Vibrational Satellite Structure. The peaks observed to the high-energy side of the electronic origin at 18 767 cm^{-1} are assigned to vibrational satellites. The corresponding energies are listed in Table 2. A series of representative modes is also marked in Figure 2a. In the energy range of lattice modes (up to ≈100 cm^{-1}), a relatively strong satellite of 32 cm^{-1} is found. It accompanies the electronic origin and each vibrational satellite. Due to its low energy it is assigned to a localized phonon.

The most important satellites are those found at 253 and 413 cm^{-1} relative to the origin. For these vibrations distinct Franck−Condon progressions are observed, for example, at 505 $cm^{-1} \approx 2 \times 253$ cm^{-1}, 759 $cm^{-1} = 3 \times 253$ cm^{-1}, etc., and at 826 $cm^{-1} = 2 \times 413$ cm^{-1}, 1236 $cm^{-1} \approx 3 \times 413$ cm^{-1} (Table 2, Figure 2a). The occurrence of a progression signifies a shift of the excited state potential hypersurface with respect to the one of the ground state along the normal coordinate of the specific vibration (for example, see refs 39−42). For the 253 cm^{-1} mode, the energy differences between adjacent members of the progression are constant up to at least the sixth member (within the experimental accuracy of ±1 cm^{-1}). Hence, the potential hypersurface may be regarded as harmonic at least up to 1500 cm^{-1} above the zero-point vibrational level. To characterize the strength of the progression, one can determine the Huang−Rhys factor S, which is related to the Franck−Condon factor.[39−41] S may be estimated using the equation S

(35) The slope of the origin peak was fitted between 18 760 and 18 600 cm^{-1} with a nonlinear least-squares fit according to the Levenberg−Marquardt algorithm (Curve-Fitting Module of Origin, Microcal. Software Inc.). The χ^2 value is about 20 times smaller for the Lorentzian fit than for the Gaussian one.

(36) Demtröder, W. *Laserspektroskopie,* 3rd ed.; Springer: Berlin, Germany, 1993.

(37) Noort, M.; Jansen, G.; Canters, G. W.; van der Waals, J. H. *Spectrochim. Acta* **1976**, *32A*, 1371.

(38) Interestingly, the singlet origin at 18 780 cm^{-1} with its homogeneous FWHM of 12 cm^{-1} fits well to the second harmonic laser line of a frequency-doubled Nd:YAG laser. This line is located at 18 783 cm^{-1} (532.4 nm). This means that without application of a tunable dye-laser it is possible to obtain a site-selectively excited triplet emission spectrum of $Pt(qol)_2$ doped in perdeuterated *n*-octane.

(39) Denning, R. G. In *Vibronic Processes in Inorganic Chemistry*; Flint, C. D., Ed.; Kluwer Academic Publishers: Dordrecht, 1989; p 111.

(40) Solomon, E. I. *Comments Inorg. Chem.* **1984**, *5*, 225.

(41) Henderson, B.; Imbusch, G. F. *Optical Spectroscopy of Inorganic Solids*; Clarendon Press: Oxford, England, 1989.

Table 2. Vibrational Energies (cm^{-1}) of the Excited ^{1}ILCT State of $Pt(qol)_2$[a]

vibrational satellites[b]	assignment
0−0 (18767)	electronic origin (^{1}ILCT)
32	lattice mode[c]
53	lattice mode[c]
76	lattice mode[c]
115	lattice mode[c]
148	
202	
253	progression-forming mode, Pt−N[d] vibration, FC[e]
413	progression-forming mode, Pt−O[d] vibration, FC
505	2 × 253
535	
578	
658	combination-forming mode
668	413 + 253
759	combination-forming mode and 3 × 253
826	2 × 413
910	658 + 253
1012	759 + 253/4 × 253
1069	658 + 413
1161	658 + 2 × 253
1171	759 + 413
1199	combination-forming mode
1236	3 × 413
1266	759 + 2 × 253/5 × 253
1309	combination-forming mode
1321	658 + 413 + 253
1377	
1415	
1453	1199 + 253
1483	658 + 2 × 413
1519	759 + 3 × 253/6 × 253
1563	1309 + 253
1585	combination-forming mode and 759 + 2 × 413
1612	1199 + 413
1706	1199 + 2 × 253
1722	1309 + 413
1771	759 + 4 × 253
1815	1309 + 2 × 253
1836	1585 + 253
1861	1199 + 413 + 253
1889	
1926	
1962	
1971	1309 + 413 + 253
1994	1585 + 413
2025	1199 + 2 × 413
2068	1309 + 3 × 253
2138	1309 + 2 × 413
2219	
2323	1309 + 4 × 253
2476	
2624	
2728	

[a] Determined from the singlet excitation spectrum of $Pt(qol)_2$ in an *n*-octane Shpol'skii matrix. $T = 1.2$ K. Accuracy ±1 cm^{-1}. Detection at 15 426 cm^{-1}. [b] Vibrational satellites relative to the electronic origin at 18 767 cm^{-1}. [c] Modes with a distinct matrix character (compare ref 19). [d] Largest atomic displacements in the corresponding normal mode at N and O, respectively. [e] FC: Modes of Franck−Condon activity.

$= v(I_v/I_{v-1})$ (low-temperature limit; v is the vibrational quantum number, and I_v is the intensity of the vth member of the progression).[40] An estimate of S from the first member of the respective progression ($v = 1$) and the electronic origin yields for the 253 cm^{-1} progression $S \approx 1.0$ and for the 413 cm^{-1} progression $S \approx 0.6$. These values are considerably larger than the value estimated for the transition between the lowest excited triplet and the ground state ($S_{max} \approx 0.2$, see section 3.4). For comparison, for metal porphines and phthalocyanines, Huang−Rhys values of less than $S \approx 0.3$ are found for the transition between the lowest excited singlet and the ground state.[37,43]

Combinations of the 253 and 413 cm^{-1} modes, respectively, with other modes occur frequently (Table 2), while the combination 253 cm^{-1} + 413 $cm^{-1} \approx 665$ cm^{-1} occurs only as a weak shoulder to the 658 cm^{-1} satellite. No other combinations of these two dominant modes could be found. Therefore, the coupling between the two modes is weak (for example, see ref 50). This fact seems to be an indication of two rather independent vibrations. It is reasonable that the modes with more Pt−N and Pt−O vibrational character, respectively, are the suitable candidates for these satellites. Indeed, Raman or infrared data of similar compounds show that the energies of Pt−N vibrations lie near 250 cm^{-1} and the energies of Pt−O vibrations near 410 cm^{-1}.[44−48] Since the 253 and 413 cm^{-1} modes are Franck−Condon active, they are totally symmetric, i.e., they have a_g symmetry (in C_{2h}) and are Raman active (compare Table 3). A recent normal coordinate analysis for $Pt(qol)_2$[49] allows us to correlate the experimentally observed modes to specific a_g in-plane normal modes involving both ligands. These modes have indeed the largest atomic displacements in the spatial regions of nitrogen (experimental value 253 cm^{-1}) and oxygen (413 cm^{-1}), respectively.

Interestingly, vibrational satellites lying in the energy range of typical ligand modes, for example, at 658, 1199, or 1309 cm^{-1}, exhibit distinctly lower intensities than the 253 and 413 cm^{-1} satellites (for a discussion of this behavior, see section 3.4).

3.4 Triplet Emission and Excitation. Figure 3a shows the emission spectrum of $Pt(qol)_2$ investigated in *n*-octane at $T =$ 1.2 K. The singlet origin at 18 767 cm^{-1} is used for a selective excitation. Thus the specific site having its triplet origin at 15 426 cm^{-1} is selected. Other sites (marked with asterisks in Figure 3a) emit only with negligible intensities. Figure 4 shows the corresponding triplet excitation spectrum for $T = 1.2$ K, which also represents a site-selective spectrum, since the detection wavenumber at 15 173 cm^{-1} fits to the 253 cm^{-1} vibrational satellite of the 15 426 cm^{-1} electronic origin.

Electronic Origin. The dominant peak at (15 426 ± 1) cm^{-1} is the line of highest energy in emission (Figure 3) and of lowest energy in excitation (Figure 4). It occurs in both emission and excitation at the same spectral position and is therefore assigned as the electronic origin. An additional confirmation of this assignment is the fact that the vibrational satellite structures are well understood with respect to this origin (see below). The origin has a half-width of 3.0 cm^{-1} in emission and 2.3 cm^{-1} in excitation, which indicates the occurrence of a small line-narrowing effect. Figure 3b shows clearly a Zeeman splitting of the electronic origin into three lines when high magnetic fields up to 12 T are applied. (The temperature of $T = 10$ K is chosen

(42) Wexler, D.; Zink, J. I.; Reber, C. In *Electronic and Vibronic Spectra of Transition Metal Complexes, Vol. 1, Top. Curr. Chem. 171*; Yersin, H., Ed.; Springer: Berlin, Germany, 1994; p 173.

(43) Huang, T.-H.; Chen, W. H.; Rieckhoff, K. E.; Voigt, E.-M. *J. Chem. Phys*. **1984**, *80*, 4051.

(44) Goldstein, M.; Mooney, E. F.; Anderson, A.; Gebbie, H. A. *Spectrochim. Acta* **1965**, *21*, 105.

(45) Larsson, R.; Eskilsson, O. *Acta Chem. Scand*. **1968**, *22*, 1067.

(46) Wootton, J. L.; Zink, J. I. *J. Phys. Chem.* **1995**, *99*, 7251.

(47) Fahmi, N.; Singh, R. V. *Trans. Met. Chem*. **1995**, *20*, 185.

(48) Nakamoto, K. *Infrared and Raman Spectra of Inorganic and Coordination Compounds*, 3rd ed.; J. Wiley & Sons: New York, 1978.

(49) Degen, J. Private communication, Universität Düsseldorf, 1996 (applying a standard SBK basis in the ab initio program "gamess" (see ref 50), version of November 1995).

(50) Schmidt, M. W.; Baldridge, K. K.; Boatz, J. A.; Elbert, S. T.; Gordon, M. S.; Jensen, J. H.; Koseki, S.; Matsunaga, N.; Nguyen, K. A.; Su, S.; Windus, T. L.; Dupuis, M.; Montgomery, J. A. *J. Comput. Chem*. **1993**, *14*, 1347.

(51) Yersin, H.; Huber, P.; Wiedenhofer, H. *Coord. Chem. Rev*. **1994**, *132*, 35.

Table 3. Vibrational Energies (cm^{-1}) of the Excited ^{3}ILCT and the Ground State of $Pt(qol)_2$

ground state vibrational satellites (emission)[a]	^{3}ILCT vibrational satellites (excitation)[a]	Raman[b]	assignment
0−0 (15426)	0−0 (15426)		electronic origin (^{3}ILCT)
31	31		lattice mode[c]
53			lattice mode[c]
76			lattice mode[c]
98			HT,[d] lattice mode[c]
113			lattice mode[c]
130			HT, lattice mode[c]
253	247	249[e]	progression-forming mode, FC,[d] Pt−N vibration[f]
277			HT
413	407	410	progression-forming mode, FC, Pt−O vibration[f]
446			HT
499	495[g]	498	combination-forming mode
507	495[g]		em, 2 × 253/exc, 2 × 247
	523		combination-forming mode
529			HT
538		538	combination-forming mode
584	575	582	combination-forming mode
667	652		em, 413 + 253/exc, 407 + 247
752			499 + 253
767		760[e]	combination-forming mode
	768		523 + 247
792			538 + 253
797			767 + 31
826			2 × 413
839			584 + 253
861			
912			499 + 413
951			538 + 413
998			584 + 413
1019			767 + 253
1084			584 + 499
1180			767 + 413
1230		1228	L[h] (1230)[i]
1329		1322[d]	L
1386		1382	combination-forming mode, L
1391			combination-forming mode, L
1468		1464	L (1468)[i]
1508		1504	L (1507)[i]
1600		1596	L (1594)[i]
1641			1386 + 253
1645			1391 + 253
1801			1386 + 413
1804			1391 + 413

[a] Determined from triplet emission and excitation spectra of $Pt(qol)_2$ in an *n*-octane Shpol'skii matrix. Accuracy ± 1 cm^{-1}. $T = 1.2$ K. Vibrational peaks relative to electronic origin at 15 426 cm^{-1}. [b] $T = 298$ K. Neat material. Measured at the Imperial College, London. [c] Modes with distinct matrix character (compare ref 19). [d] HT: modes of Herzberg−Teller activity. FC: modes of Franck−Condon activity. [e] Tentative correlation. [f] Largest atomic displacements in the corresponding normal mode at N and O, respectively. [g] Assignment deduced from the intensity distribution of the 247 cm^{-1} progression. [h] L: ligand vibrational mode. [i] Vibrational energy found for $Pd(qol)_2$ (spectrum not reproduced).

to avoid freezing out the higher lying triplet components at higher magnetic fields.) This phenomenon represents an obvious confirmation of the triplet character of the emitting state. In the investigated range above $B = 1$ T the splitting is linear in B exhibiting a slope of (0.93 ± 0.04) cm^{-1}/T. The linearity displays the high-field situation. The *g*-factor is determined to be 2.0, which represents almost the pure spin value. (The triplet character of the origin at 15 426 cm^{-1} is further displayed in the relatively long luminescence decay time at $T = 1.2$ K. The longest decay component is 60 μs. For details of the decay behavior, see below.) The zero-field splitting (zfs) could not be resolved, and thus it must be smaller than about 1 cm^{-1}. This is an important result, since it demonstrates that Pt 5d-orbital contributions which introduce high spin−orbit coupling are small. Otherwise a larger zfs would be expected. Therefore, an assignment of this triplet to a ^{3}MLCT state, which usually exhibits a large zfs, is excluded. (For details concerning zfs and metal d-contributions, see refs 11, 12, and 51). This result is in good accord with the assignment of the lowest triplet as being mainly a ligand-centered state. However, the fact that the transition carries enough oscillator strength to allow a direct excitation (triplet excitation spectra can be registered) points to the occurrence of some small singlet admixtures to the triplet, induced by spin−orbit coupling from the metal. Presumably, the coupling of metal character to the ligand-centered states is not sufficient to overcome distortions individually experienced by the different ligands. Thus, it is likely that the triplet state is not delocalized over the two ligands (compare the discussion for $[Ru(bpy)_3]^{2+}$ and related compounds in ref 12).

A careful and highly sensitive search for further electronic transitions in the energy range between the triplet state at 15 426 cm^{-1} and the ^{1}ILCT at 18 767 cm^{-1} did not reveal any additional electronic state (plot not reproduced). Thus, it may be concluded that the two states identified are the singlet and the triplet having (nearly) the same orbital parentage, and therefore, the triplet may be characterized as a ^{3}ILCT state. This assignment is further supported by the amount of 3341 cm^{-1} observed for the energy difference between these states. This singlet−triplet separation which is essentially determined by the exchange interaction seems to have the right magnitude for CT states.[52]

Vibrational Satellite Structures. The triplet emission and excitation spectra (Figures 3 and 4) both exhibit highly resolved

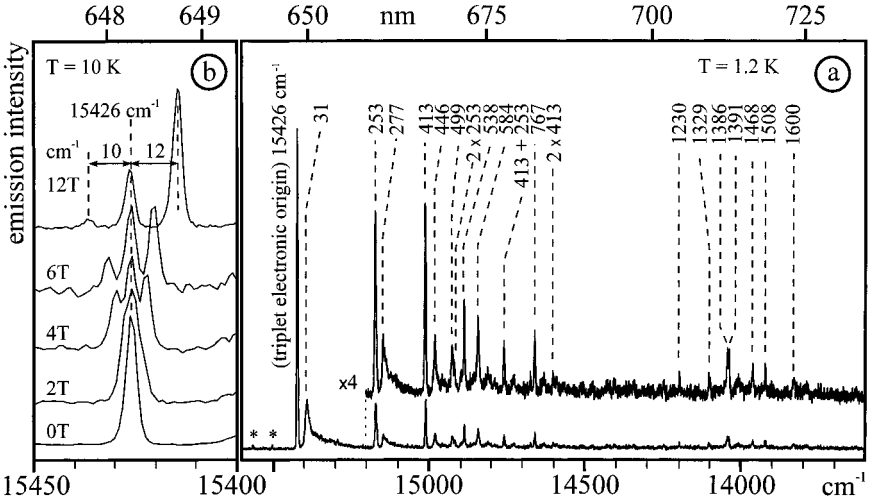

Figure 3. (a) Triplet (^{3}ILCT) emission spectrum of Pt(qol)$_2$ in an *n*-octane Shpol'skii matrix at $T = 1.2$ K. Due to the selective excitation at 18 767 cm^{-1} (electronic origin of the ^{1}ILCT state) a specific site is investigated. Spectral resolution: 0.6 cm^{-1}. Vibrational satellites are specified relative to the electronic origin at 15 426 cm^{-1}. The asterisks indicate residual intensities of origins of different sites (see Table 1). (b) Emission spectra in the range of the triplet origin for different magnetic fields (expanded; $T = 10$ K). The intensities are not comparable.

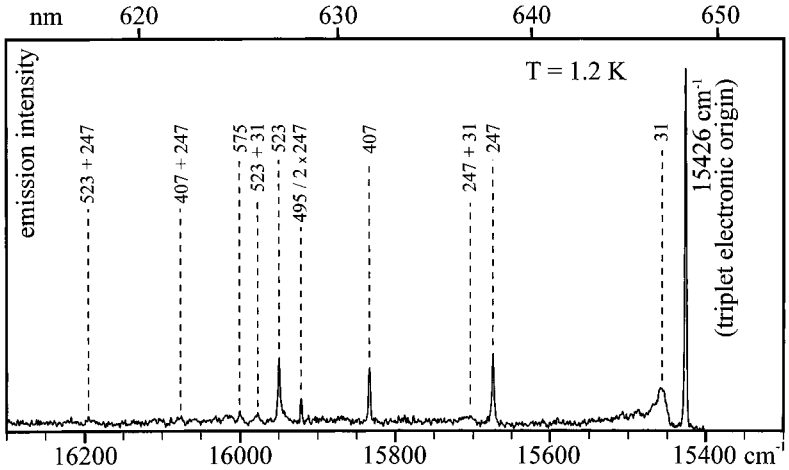

Figure 4. Triplet (^{3}ILCT) excitation spectrum of Pt(qol)$_2$ in an *n*-octane Shpol'skii matrix at $T = 1.2$ K. Due to the selective detection at 15 173 cm^{-1} (253 cm^{-1} vibrational satellite to the electronic origin at 15 426 cm^{-1}) a specific site is investigated. Spectral resolution: 0.5 cm^{-1}. The vibrational satellites are specified relative to the electronic origin at 15 426 cm^{-1} (see Table 3). The spectrum is not corrected with respect to the characteristic of the laser dye (DCM).

patterns, which are, aside from the electronic origin, assigned to phonon and vibrational satellite structures. A phonon satellite of 31 cm^{-1} (which can be correlated to the 32 cm^{-1} satellite found in the singlet excitation spectrum) occurs in the triplet emission and the triplet excitation spectra. However, its intensity relative to the origin is much weaker than found in the singlet excitation spectrum. This is indicative of differences in coupling properties of the excited singlet and triplet states, respectively, with the *n*-octane matrix. In Table 3, the energies of the vibrational modes are compared to Raman data. A good correlation between emission, excitation, and Raman lines is obvious. However, the vibrational energies of the ground state (from emission) and the ^{3}ILCT state (from excitation) are slightly different. The red shifts observed for the modes in the ^{3}ILCT state with respect to those of the ground state display slightly smaller vibrational force constants in the ^{3}ILCT. However, the amount of red shift of the vibrational energies (about 2%) may be regarded as being relatively small (compare also refs 13 and 14).

In section 3.3 it was shown that modes occurring at 253 and 413 cm^{-1} in the ^{1}ILCT state may be characterized as largely exhibiting Pt−N and Pt−O vibrational character, respectively. These modes correspond to the 253 and 413 cm^{-1} modes (ground state) and the 247 and 407 cm^{-1} modes (^{3}ILCT state), respectively. Interestingly, the transitions between ^{3}ILCT and the ground state do not show any pronounced Franck−Condon progressions, in either emission or excitation. The largest value of the Huang−Rhys factor S can be estimated to be $S \approx 0.2$, which is significantly smaller than found for the transition from the ground state to the ^{1}ILCT state (see section 3.3). This shows that the potential hypersurfaces of the ^{3}ILCT state have appreciably smaller shifts than the ^{1}ILCT surfaces relative to the ones of the ground state.

The intensities of the vibrational satellites in the energy range of typical ligand modes (≈600 to ≈1700 cm^{-1}) are relatively weak compared to those involving the Pt−N and the Pt−O modes, respectively (Figure 3a). This behavior can be explained as follows: In particular those specific vibrational modes which are connected to spatial regions of the chromophore that experience distinct changes of charge density upon an electronic transition are often observed as intense vibrational satellites in emission or excitation spectra (for a detailed discussion, see refs 53 and 54). Consequently, it can be deduced that the spatial

(52) Turro, N. J. *Modern Molecular Photochemistry*, 1st ed.; The Benjamin/Cummings Publishing Co. Inc.: California, 1978; p 31.

(53) Braun, D.; Huber, P.; Wudy, J.; Schmidt, J.; Yersin, H. *J. Phys. Chem.* **1994**, *98*, 8044.

(54) Gastilovich, E. A. *Sov. Phys. Usp.* **1991**, *34*, 592.

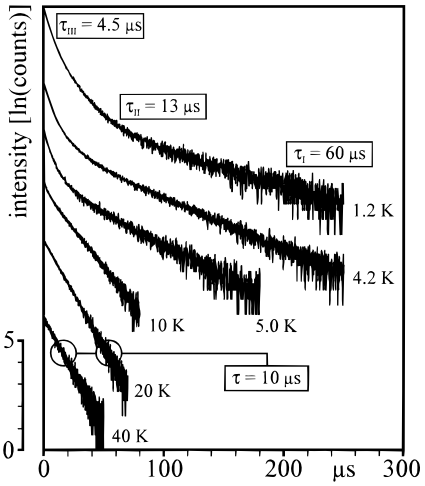

Figure 5. Phosphorescence decay curves of Pt(qol)$_2$ in an *n*-octane Shpol'skii matrix for different temperatures. Excitation at ≈29 670 cm^{-1} (337.1 nm). Detection at 15 426 cm^{-1} (electronic origin ^{3}ILCT). The decay at $T = 1.2$ K is triexponential. The decay components given result from least-squares fits.

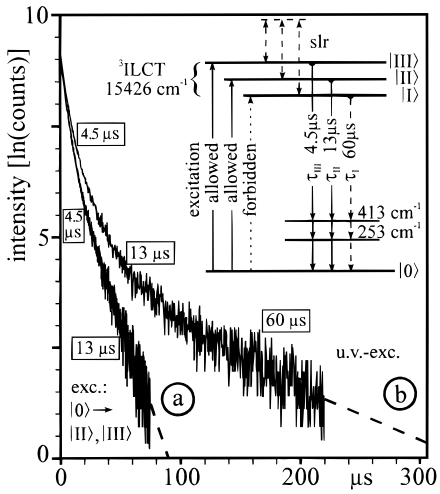

Figure 6. Phosphorescence decay of Pt(qol)$_2$ in an *n*-octane Shpol'skii matrix at $T = 1.2$ K. To avoid a resonant detection the phosphorescence is registered at 15 013 cm^{-1} (413 cm^{-1} vibrational satellite to the ^{3}ILCT electronic origin at 15 426 cm^{-1}). (a) Excitation at 15 426 cm^{-1} (electronic origin of the ^{3}ILCT state). (b) Excitation at ≈29 670 cm^{-1} (337.1 nm). The inset shows an energy level scheme for the triplet sublevels |I(^{3}ILCT)⟩, |II(^{3}ILCT)⟩, and |III(^{3}ILCT)⟩ which are not resolved spectrally, zfs < 1 cm^{-1}. The energy order is arbitrary. The excitation from the ground state to |I(^{3}ILCT)⟩ is strongly forbidden. Note that the 60 μs component is absent with excitation into the ^{3}ILCT origin.

region of the two-ring heterocycle, which is the main origin of the typical high-energy ligand modes, is not so strongly involved in the process of charge reorganization according to the transitions between ground state and ^{1,3}ILCT as are the spatial regions of oxygen and nitrogen. Such a behavior is expected for this type of ILCT transition in which the strongest changes of charge density occur in the regions of oxygen and nitrogen.

For completeness it is mentioned that Pt(qol)$_2$ investigated in the *perdeuterated n*-octane-d_{18} matrix exhibits a vibrational satellite structure very similar to that found for the protonated matrix with respect to intensities and energies. (For an example with distinct differences see ref 19.)

Phosphorescence Decay and Spin−Lattice Relaxation. Figure 5 presents phosphorescence decay curves of Pt(qol)$_2$ for different temperatures. The compound was excited into a higher lying singlet ($\lambda_{exc} = 337.1$ nm; similar results yield the excitation into the ^{1}ILCT origin at 532.85 nm). At $T = 1.2$ K, the emission decays triexponentially with the components $\tau_I = (60 \pm 4)$ μs, $\tau_{II} = (13 \pm 1)$ μs, and $\tau_{III} = (4.5 \pm 0.5)$ μs according to the three independently emitting sublevels |I(^{3}ILCT)⟩, |II(^{3}ILCT)⟩ and |III(^{3}ILCT)⟩. (The designation of the triplet sublevels does not indicate an energy order. This order is not known since the individual sublevels could not yet be resolved spectrally.) At $T = 1.2$ K, the initial spin polarization obtained by a specific population of the sublevels via the process of intersystem crossing is preserved. With increasing temperature the decay behavior changes drastically due to an increasing spin−lattice relaxation (slr) between the sublevels (see the decay curves for $T = 4.2$, 5.0, and 10 K). A thermalization is reached near 20 K, when the decay is monoexponential with a lifetime of $\tau = (10 \pm 1)$ μs. An average decay time τ_{av} can be calculated from the three low-temperature values. Using $\tau_{av} = 3/(\tau_I^{-1} + \tau_{II}^{-1} + \tau_{III}^{-1})$, one obtains 9.5 μs (for example, compare refs 19 and 55). This value is in good agreement with the experimentally determined one and thus confirms that the decay components measured at $T = 1.2$ K are the intrinsic lifetimes of the three triplet sublevels of one chromophore. For completeness it is mentioned that the nonthermalization between closely spaced energy levels at low temperature is well-known for organic compounds (representing the basis for ODMR spectroscopy, for example, see ref 58), but this behavior has only recently been discussed in detail for transition metal complexes with organic ligands.[11−14,19,59,60] The mechanism of slr is not further investigated in this contribution. However, it is noted that according to the small zfs a *direct process* involving one phonon will not be of relevance but *Raman* and/or *Orbach* processes should be taken into account.[19,41,61]

For comparison, the situation in the perdeuterated matrix should be mentioned. Interestingly, one observes exactly the same decay behavior as in the protonated matrix (detection at the triplet electronic origin at 15 437 cm^{-1}, see Table 1). In contrast to this situation, other compounds like *cis*-Pd(2-thpy)$_2$ (2-thpy$^-$: C-deprotonated form of 2-thienylpyridine) exhibit different decay components in perdeuterated and perprotonated matrices, respectively.[19] This behavior indicates a relatively small influence of the matrix on the ^{3}ILCT of Pt(qol)$_2$.

Selective Excitation of Individual Triplet Sublevels. Interestingly, a direct excitation of the lowest triplet of Pt(qol)$_2$ at 15 426 cm^{-1} is possible. Figure 6a shows that in this situation at $T = 1.2$ K the phosphorescence is found to decay *biexponentially*, exhibiting two short components of 4.5 and 13 μs. These values just correspond to τ_{II} and τ_{III} (see above). It is important that *no* long-lived component (τ_I) could be detected, contrary to the situation with a UV excitation into a higher lying singlet where three decay components occurred (compare Figure 6a and Figure 6b). This means that the triplet sublevels |II(^{3}ILCT)⟩ and |III(^{3}ILCT)⟩ are populated selectively while sublevel |I(^{3}ILCT)⟩ cannot be excited directly, since the corresponding transition probability is too small. Due to the slow processes of spin−lattice relaxation at $T = 1.2$ K, the spin polarization is preserved during the emission lifetime. However, with temperature increase, state |I(^{3}ILCT)⟩ will be populated and an additional long emission component appears (not shown in Figure 6). At $T = 1.2$ K, the |I(^{3}ILCT)⟩ can be populated

(55) Tinti, D. S.; El-Sayed, M. A. *J. Chem. Phys.* **1971**, *54*, 2529.
(56) Yamauchi, S.; Azumi, T. *J. Chem. Phys.* **1977**, *67*, 7.
(57) Schwoerer, M.; Sixl, H. *Z. Naturforsch.* **1969**, *24*, 952.
(58) Clarke, R. H., Ed. *Triplet State ODMR Spectroscopy*; Wiley: New York, 1982.
(59) Yersin, H.; Braun, D. *Coord. Chem. Rev.* **1991**, 111, 39.
(60) Griesbergen, C.; Glasbeek, M. *J. Phys. Chem.* **1993**, *97*, 9942.
(61) Scott, P. L.; Jeffries, C. D. *Phys. Rev.* **1962**, *127*, 32.

by processes of intersystem crossing after an excitation into an excited singlet (Figure 6b). Thus, both processes, temperature increase and UV excitation, lead to triexponential decay curves. Corresponding properties have also been observed for a series of other transition metal compounds, like Pd(2-thpy)$_2$, Pt(bpy)$_2^{2+}$, and Pt(2-thpy)$_2$.[20,62a,b] This interesting behavior allows us to study the mechanisms of spin−lattice relaxation and further relaxation paths in detail.

The different decay times observed for the three triplet sublevels of Pt(qol)$_2$ at $T = 1.2$ K (when using UV excitation) make it possible to separate the emission spectra which result from the different sublevels by time-resolved spectroscopy. Similar experiments have already been carried out for other transition metal compounds (for example, see ref 20). For Pt(qol)$_2$, the short-lived spectrum measured with a time window up to 50 μs after the excitation pulse carries most of the emission intensity of the sublevels $|\mathrm{II}(^3\mathrm{ILCT})\rangle$ and $|\mathrm{III}(^3\mathrm{ILCT})\rangle$. It is totally different compared to the long-lived one (for example, registered with a time delay of 100 μs and a time window of 300 μs). The spectra are not reproduced here, but the main message is that the short-lived emission spectrum is largely the same as the time-integrated one shown in Figure 3. This implies that the usual, time-integrated emission is strongly dominated by the emission from the states $|\mathrm{II}(^3\mathrm{ILCT})\rangle$ and $|\mathrm{III}(^3\mathrm{ILCT})\rangle$. On the other hand, the delayed and long-lived emission stemming from the $|\mathrm{I}(^3\mathrm{ILCT})\rangle$ sublevel shows a number of vibrational satellites which (nearly) do not occur in the time-integrated emission spectrum. For example, one finds satellites at 98, 130, 277, 446, and 529 cm^{-1}. Relative to the electronic origin, these satellites are much more intense than found in the short-lived spectrum. Consequently, these specific vibrational modes are assigned to represent vibronically coupling modes which supply additional radiative decay paths from state $|\mathrm{I}(^3\mathrm{ILCT})\rangle$ to the ground state by Herzberg−Teller processes (compare refs 12, 14, 20, 54, and 63). These coupling pathways probably include mainly spin-vibronic mechanisms.[63,64]

4. Characterization of the Lowest Excited States of Pt(qol)$_2$. A Concluding Summary

Pt(qol)$_2$ is investigated in an *n*-octane Shpol'skii matrix. It is possible to obtain highly resolved excitation spectra of the lowest excited singlet state and emission as well as excitation spectra of the lowest triplet state. The spectra are by a factor of about 400 better resolved than hitherto known and thus provide an enormous increase of information which can be used for a classification of the states involved.

The electronic origin of the transition from the singlet ground state to the lowest excited singlet lies at 18 767 cm^{-1}. The singlet assignment is strongly supported by the magnetic field behavior of the resolved origin structure. This electronic transition is identified to be responsible for the intense low-energy singlet absorption near 21 000 cm^{-1} of Pt(qol)$_2$ dissolved in DMF. To energies lower than this electronic singlet transition one can exclude the occurrence of any other electronic transition besides the lowest triplet at 15 426 cm^{-1}. Thus, it is concluded that these states possess to a first approximation the same orbital parentage. The energy difference between triplet and singlet states of about 3340 cm^{-1}, being essentially given by the exchange interaction, is much too small for a typical $\pi\pi^*$ transition of a conjugated two-ring aromatic compound but fits well to a charge transfer (CT) transition. In fact, two types of CT transitions have been suggested for the triplet, metal to ligand charge transfer (MLCT)[4] and intraligand charge transfer (ILCT)[3], respectively. Keeping in mind that typical ^{3}MLCT states exhibit relatively large zero-field splittings (zfs, for example, 61 cm^{-1} for $[\mathrm{Ru(bpy)_3}]^{2+}$ and 210 cm^{-1} for $[\mathrm{Os(bpy)_3}]^{2+}$),[11,12,51] this type of transition can be ruled out, since the lowest triplet state of Pt(qol)$_2$ has a zfs smaller than 1 cm^{-1}. But for a ^{3}ILCT state which is mainly confined to an organic ligand such a small splitting is expected. Thus, the lowest excited singlet and the lowest triplet may be specified as being mainly of ^{1}ILCT and ^{3}ILCT character, respectively. However, a small Pt 5d-orbital contribution manifests itself in the relatively large rates of intersystem crossing from ^{1}ILCT to ^{3}ILCT, and also in the radiative decay rate of the two sublevels $|\mathrm{II}(^3\mathrm{ILCT})\rangle$ and $|\mathrm{III}(^3\mathrm{ILCT})\rangle$. In particular, this results in the possibility of their direct excitation.

The well-resolved vibrational satellite structures provide further support for the classification given above. In particular, the fact that the Pt−N and the Pt−O vibrational satellites dominate all spectra indicates that changes of charge densities upon excitation occur mainly in the spatial regions of oxygen and nitrogen for singlet *and* triplet. This leads to an appreciable change of the equilibrium positions of the potential hypersurfaces in the ^{1}ILCT state compared to those of the ground state along the corresponding normal coordinates. (The Huang−Rhys factor S characterizing this property is of the order of 1 for the metal−ligand modes at 253 and 413 cm^{-1}.) Interestingly, the force constants corresponding to these modes are (within the limits of experimental error) just the same in the ground state and in the ^{1}ILCT state.

Although the dominance of the two vibrational satellites with Pt−N and Pt−O character is also obvious for the ^{3}ILCT state, one observes a somewhat different behavior. The vibrational energies are slightly smaller in the excited triplet state (247 and 407 cm^{-1}) than in the ground state (253 and 413 cm^{-1}), and the equilibrium positions of the potential hypersurfaces of the ^{3}ILCT are distinctly less shifted relative to those of the ground state ($S \approx 0.2$) than found for the ^{1}ILCT. Obviously, both states experience different admixtures of higher lying states with other orbital parentage. But it should also be taken into account that singlets and triplets are described by wavefunctions of different symmetries. In particular, electrons in the triplet state have a larger average separation than in the corresponding singlet. This results in different electron charge distributions and therefore can lead to different geometries for the ^{3}ILCT state compared to the ^{1}ILCT state.

Acknowledgment. Financial support of the "Fonds der Chemischen Industrie" and the "Deutsche Forschungsgemeinschaft" is gratefully acknowledged. We thank Prof. Dr. W. P. Griffith and Dr. T. Y. Koh (Imperial College, London) and the University of London Intercollegiate Research Service (ULIRS) for measuring the Raman spectra. We also thank Priv. Doz. Dr. J. Degen (Universität Düsseldorf) for carrying out the normal coordinate analysis and making it accessible for us prior to publication. J.K.N. thanks Bowdoin College for sabbatical leave support and the Fulbright Foundation for a Fulbright scholar award.

IC9609463

(62) (a) Yersin, H.; Strasser, J. *J. Lumin.*, in press. (b) Schmidt, J.; Strasser, J.; Yersin, H. *Inorg. Chem.*, in press.
(63) Albrecht, A. C. *J. Chem. Phys.* **1963**, *38*, 354.
(64) Braun, D.; Hensler, G.; Gallhuber, E.; Yersin, H. *J. Phys. Chem.* **1991**, *95*, 1067.